Anatomy of perpendicular magnetic anisotropy in Fe/MgO magnetic tunnel junctions: First-principles insight

A. Hallal, H. X. Yang, B. Dieny, and M. Chshiev*

SPINTEC, UMR CEA/CNRS/UJF-Grenoble 1/Grenoble-INP, INAC, 38054 Grenoble, France

(Received 13 August 2013; revised manuscript received 15 October 2013; published 21 November 2013)

Using first-principles calculations, we elucidate microscopic mechanisms of perpendicular magnetic anisotropy (PMA) in Fe/MgO magnetic tunnel junctions through evaluation of orbital and layer resolved contributions into the total anisotropy value. It is demonstrated that the origin of the large PMA values is far beyond simply considering the hybridization between Fe-3d and O-2p orbitals at the interface between the metal and the insulator. Onsite projected analysis shows that the anisotropy energy is not localized at the interface but it rather propagates into the bulk showing an attenuating oscillatory behavior which depends on orbital character of contributing states and interfacial conditions. Furthermore, it is found in most situations that states with $d_{yz(xz)}$ and d_{z^2} character tend always to maintain the PMA while those with d_{xy} and $d_{x^2-y^2}$ character tend to favor the in-plane anisotropy. It is also found that while MgO thickness has no influence on PMA, the calculated perpendicular magnetic anisotropy oscillates as a function of Fe thickness with a period of 2 ML and reaches a maximum value of 3.6 mJ/m^2.

DOI: 10.1103/PhysRevB.88.184423 PACS number(s): 75.30.Gw, 72.25.Mk, 75.70.Cn, 75.70.Tj

Perpendicular magnetic anisotropy (PMA) at ferromagnetic transition-metal/insulator interfaces has become of huge interest in the context of development of various spintronic devices based on spin-transfer (STT) or spin-orbit torques (SOT). In particular, out-of-plane magnetized magnetic tunnel junctions (pMTJ) are now intensively developed for STT magnetic random access memories (STT-MRAM) applications where the strong PMA originating from the CoFe/MgO interface allows us to maintain the thermal stability of the storage layer magnetization down to at least the 20-nm technological node.[1–9] This interest is due to the fact that it makes it possible to avoid introducing within or next to the ferromagnet heavy nonmagnetic elements which were believed to be essential to trigger the PMA thanks to their large spin-orbit coupling (SOC).[10–14] However, introducing heavy elements is detrimental for STT-based devices since their large SOC tends to increase Gilbert damping, resulting in an increase of critical current required for switching the storage layer magnetization. The interfacial PMA at CoFe/MgO interface is remarkably large despite the weak SOC. Indeed, PMA with large values around 1 to 2 mJ/m^2 were reported at Co(Fe)/MOx interfaces (M = Mg, Al, etc.).[6,15–17] These values are comparable to those observed at the Co/Pt interface which is considered as a reference for large interfacial anisotropy.[14] It was observed by x-ray photoemission (XPS) and absorption experiments[18] that interfacial PMA at ferromagnetic metal/oxide gets maximum when oxygen is present along the metal/oxide interface so that chemical bounds (hybridization) can form between orbitals of metallic ions and oxygen. Because of this remarkable combination of large anisotropy and weak SOC, this phenomenon is now widely used in pMTJs for high density STT-MRAM.[8,9]

This phenomenon attracted a large attention from theoretical point of view. Using first-principles calculations, several groups addressed magnetic anisotropy in Fe/MgO interfaces and reported values between 1 and 2 mJ/m^2 for pure Fe/MgO interfaces.[20–22] It was also found that in overoxidized or underoxidized interfaces, the PMA values decrease,[21–24] in good agreement with experimental observations.[15,16,18,25,26]

Although PMA has been extensively studied both experimentally and theoretically, the origin of its large value with such weak SOC system has not yet been fully unveiled. The large PMA in (Co)Fe/MgO(AlOx) is usually interpreted in terms of strong hybridizations between interfacial (Co)Fe-3d and the O-2p orbitals combined with SOC.[8,22,27] This interpretation leads to a picture in which the PMA is mostly localized at the interface. However, only a slight to moderate decrease of PMA was reported in underoxidized case when the oxygen is removed from the interface,[22] suggesting that other contributions exist aside from the hybridization between Fe and O orbitals. Therefore, the origin of the large PMA in Fe/MgO seems to be more complex.

In this paper, we investigate the PMA evolution as a function of the Fe and MgO layer thicknesses and different interfacial conditions using first-principles calculations. In order to elucidate the microscopic mechanisms of PMA, we employ onsite projected analysis of PMA which enables identification not only of each layer's contribution to the total PMA, but also from states with different orbital characters. It is then illustrated that the PMA energy is not localized at the interface of Fe/MgO but rather distributed into the bulk with a damped oscillatory behavior as a function of distance from the interface. By analyzing interfacial and bulk contributions into the total PMA value, we conclude that the PMA has a more complex origin. The Fe-O bonding picture is an oversimplification of the anisotropy mechanism. It only contributes by a fraction of the total PMA value. Furthermore, states with $d_{yz(xz)}$ and d_{z^2} character tend to contribute positively to the PMA while those with d_{xy} and $d_{x^2-y^2}$ character favor in-plane anisotropy. Moreover, while MgO thickness has no influence on PMA, it is found to oscillate as a function of Fe thickness with a period of 2 monolayers (ML) and reaches a maximum of 3.6 mJ/m^2.

Our first-principles calculations were performed using the VASP package[28–30] following the approach in Ref. 22. We use 11 ML of MgO and 7 ML of Fe for all five structures considered as shown in Fig. 1: (V) Fe_7/vacuum, (O) overoxidized interface (with O inserted at the interfacial

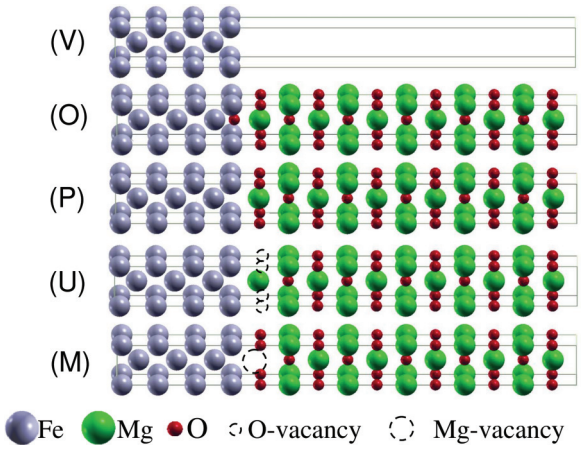

FIG. 1. (Color online) Schematics of the calculated crystalline structures for (V) Fe/Vacuum, (O) overoxidized Fe_7/MgO_{11}, (P) pure Fe_7/MgO_{11}, (U) underoxidized Fe_7/MgO_{11}, and (M) Mg vacancy in Fe_7/MgO_{11}. Fe, Mg, and O are represented by silver, green, and red balls, respectively.

magnetic layer), (P) "pure" interface, (U) underoxidized interface for investigation of oxidation conditions effects, and (M) Mg vacancy at the interface. We introduce the orbital and layer resolved magnetic anisotropy as $MA_{O,L} = \frac{-1}{a^2}(E^{\perp}_{O,L} - E^{\parallel}_{O,L})$ where a is the in-plane lattice constant and $E^{\perp(\parallel)}_{O,L}$ represents the energy contribution into anisotropy from layer L and orbital O for out-of-plane (in-plane) magnetization orientation in respect to the Fe/MgO interface. Positive values correspond to out-of-plane anisotropy. Taking into account that magnetocrystalline anisotropy of bulk iron is negligible, the interfacial anisotropy K_S for the whole structure can be defined as $K_S = \sum_{O,L} MA_{O,L}$ where the sum is taken over all orbitals and layers of the Fe. Systematic calculations with Fe (respectively MgO) thickness varied between 5 and 13 ML with a fixed 11 ML of MgO (respectively Fe) for the odd number of monolayers. For even number of MLs, Fe thickness was varied between 6 and 12 MLs with a fixed 10-ML thickness of MgO.

In Fig. 2, the surface anisotropy K_S shows an oscillatory behavior as a function of Fe thickness t_{Fe} with a period of 2 ML. The amplitude of K_S increases linearly for odd number of layers and reaches a maximum of 3.5 $\mathrm{mJ/m^2}$ at 9 ML of Fe thickness. At the same time for even number, it reaches a maximum value of 3.6 $\mathrm{mJ/m^2}$ at 8 ML of Fe and then decreases for higher thicknesses. Figure 2 also shows the effective anisotropy $K_{\mathrm{eff}}t_{\mathrm{Fe}}$ dependence on Fe thickness where K_{eff} is usually defined as $K_{\mathrm{eff}} = K_S/t_{\mathrm{Fe}} - 2\pi M_s^2$ with the second term representing the demagnetizing energy which favors in-plane anisotropy (M_s is Fe layer's saturation magnetization). However, since we are dealing with thin Fe films, we found that the demagnetization energy calculated from $2\pi M_s^2$ is underestimated by 30% compared to the one evaluated from the magnetostatic dipole-dipole interaction.[19] Therefore, in this work, K_{eff} is defined as $K_{\mathrm{eff}} = K_S/t_{\mathrm{Fe}} - E_{\mathrm{demag}}$ where E_{demag} is the sum of all the magnetostatic dipole-dipole interactions up to infinity. Since K_S and K_{eff} are related, $K_{\mathrm{eff}}t_{\mathrm{Fe}}$ also shows the same oscillatory behavior. However, $K_{\mathrm{eff}}t_{\mathrm{Fe}}$ decreases and reaches the cross point around 12 Å due

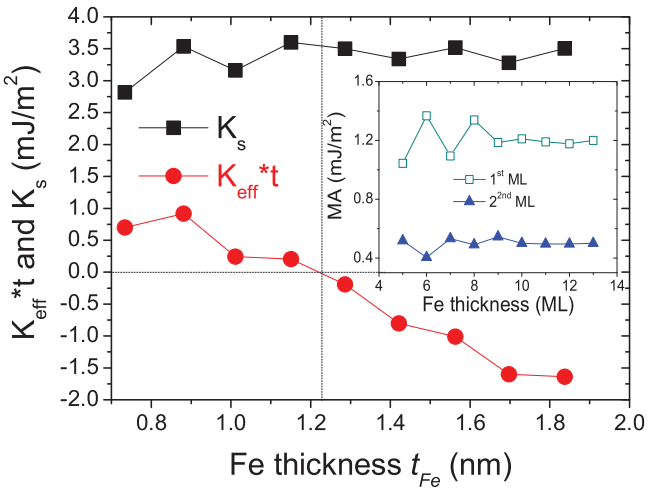

FIG. 2. (Color online) Dependencies of effective and surface anisotropy on Fe thickness for Fe/MgO/Fe MTJ, where MgO thickness is fixed to 11 ML and Fe varies from 5 to 13 ML. (Inset) Onsite projected PMA for the first and second interfacial layers as a function of Fe thickness.

to the fact that the demagnetizing energy increases with the Fe thickness (in the case where the demagnetization energy is defined by $2\pi M_s^2$, the cross point is found to be around 16 Å). In recent experiments, the cross point was found around 5 Å for the Cr(V)/Fe/MgO system.[31] This discrepancy between experiment and calculation is due to the fact that our structures have two Fe/MgO interfaces and thus the cross point in the case of one Fe/MgO interface should be around 6 Å, which is in agreement with the experimental findings.

In order to understand the origin of PMA behavior as a function of Fe thickness, we investigated the onsite projected magnetic anisotropy for different thicknesses shown in Fig. 3 (top panel). One can see that the main contribution is localized at the first interfacial Fe layer and this value increases slightly as we increase the Fe thickness and reaches a maximum of

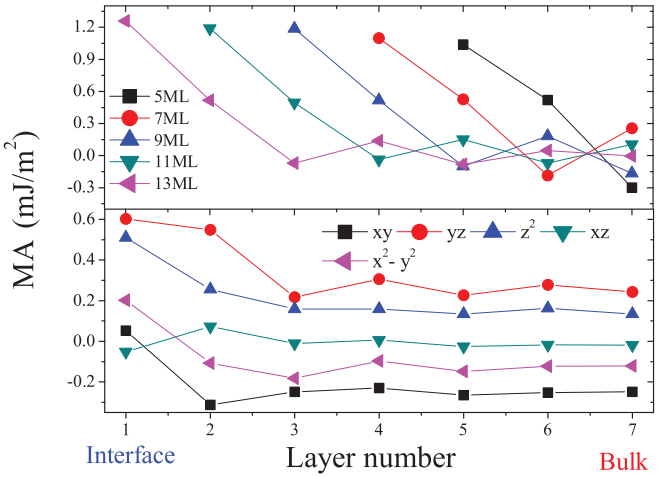

FIG. 3. (Color online) (Top panel) Onsite projected magnetic anisotropy for different Fe thicknesses in the Fe/MgO system. The curves are shifted with respect to each other for clarity. (Bottom panel) d-orbital resolved contribution to PMA as a function of layer number for $Fe_{13}[MgO_{11}]$.

TABLE I. Surface anisotropy K_S in mJ/m^2 for all the considered structures and corresponding contributions of the first two layers next to the interface. The K_S values are given for two interfaces.

Structure	PMA	K_S	$MA_{o,1} + MA_{o,2}$
$Fe_7[MgO]_{11}$	Pure	3.15	1.63
(MTJ)	Underoxidized	2.84	1.22
	Overoxidized	0.25	−1.56
	Mg vacancy	3.15	1.39
$Fe_7[MgO]_{11}$	Pure	2.70	1.82
(Vacuum)	Underoxidized	2.08	1.17
	Overoxidized	−0.33	−1.45
$Fe_7[MgO]_1$	Pure	2.62	1.85
(Vacuum)	Underoxidized	2.11	1.17
	Mg vacancy	1.20	0.65
Fe_7 (Vacuum)		1.74	0.80

1.2 mJ/m^2. At the same time, for even number of layers, the main contribution which is also localized at the interface decreases as a function of Fe thickness from 1.4 mJ/m^2 to 1.2 mJ/m^2 (inset of Fig. 2). This value (1.2 mJ/m^2) is consistent with that obtained by K. Nakamura *et al*. where one Fe atomic layer was used in calculations.[20] The second largest contribution to PMA comes from the second layer from the interface. This contribution around 0.5 mJ/m^2 shows also 2-ML oscillations period as a function of Fe thickness (inset Fig. 2).

More generally, it is observed that although the PMA takes its origin at the Fe/MgO interface, significant contributions to the PMA energy come from the next several monolayers into the bulk Fe layers exhibiting attenuated oscillatory behavior as a function of distance to the interface[32] yielding almost negligible contribution from the bulk itself.[33] Such oscillatory behavior has been recently reported experimentally and theoretically in different systems[34–36] and attributed to quantum well oscillations in a minority-spin d band at the Fermi level. As one can see from Fig. 3 (bottom panel) where orbital resolved contributions to the magnetic anisotropy are shown, Fe $d_{xz,yz}$ orbitals (from minority electrons) are dominating in PMA and seem to be at the origin of these 2-ML oscillations.

So far, we discussed the case of pure interface represented in Fig. 1 (P). We now present results of the impact of interfacial conditions for different configurations and structures represented in Fig. 1 (V, U, O, M). In Table I, we summarize K_S and $MA_{o,1} + MA_{o,2}$ values since the latter represent the main contribution to K_S as explained above.[37] The calculations show that PMA reaches its maximum in the case of pure interfaces for all structures considered. The PMA is slightly reduced compared to the pure case for underoxidized interfaces and strongly reduced (or disappear) for overoxidized interfaces in agreement with previous reports.[22,25,26] For slab structures comprising both Fe/MgO and Fe/vacuum interfaces [Fe(001) surface], we obtained 2.7 mJ/m^2 for $Fe_7[MgO]_{11}$ which is in agreement with the previous report of 2.85 mJ/m^2 for the $Fe_9[MgO]_9$ slab.[21] Furthermore, we also investigated the PMA dependence on MgO thickness and found that K_S is not affected by it varying in all cases by less than ±0.1 mJ/m^2

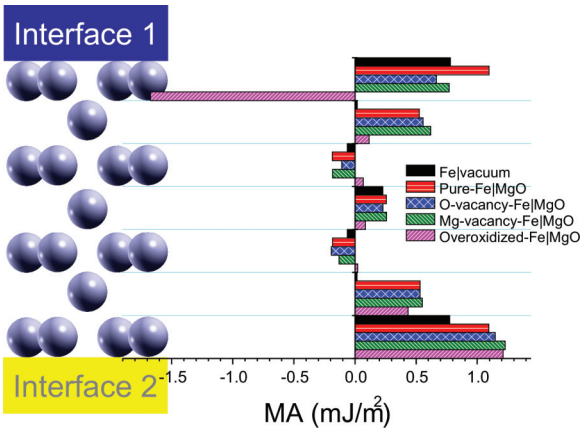

FIG. 4. (Color online) Onsite projected magnetic anisotropy for different interface 1/Fe_7/interface 2 structures. Interface 1: Fe_7/vacuum, pure $Fe_7[MgO]_{11}$, underoxidized $Fe_7[MgO]_1$1 (O vacancy), Mg vacancy Fe_7/MgO, and over-oxidized $Fe_7[MgO]_{11}$. Interface 2: Fe_7/vacuum and pure Fe_7/MgO_{11}.

which is in agreement with experiments.[38] For example, 1 ML of MgO on top of 7 ML of Fe gives rise to PMA of 2.62 mJ/m^2 which is comparable with case of 11 ML of MgO as seen in Table I. Interestingly, Table I shows that while the PMA is relatively insensitive to MgO thickness in the pure and underoxidized cases, this is no longer the case when Mg vacancies are present. The latter significantly affect the PMA for thin MgO layers as seen for the Fe_7/MgO_1 structure.

In order to elucidate the influence of interfacial conditions on PMA, in Fig. 4 we summarize onsite projected magnetic anisotropy contributions from each individual Fe layer sandwiched between interface 1 considering the various investigated cases (see Fig. 1) and interface 2 being kept either Fe/vacuum or pure Fe/MgO. By analyzing data presented in Fig. 4, one can identify several mechanisms of the interfacial PMA and separate them in three main origins.[39] The first one originates from the symmetry breaking at the Fe/vacuum interface case and one can see that the main contribution to the total PMA of pure Fe slab (0.87 mJ/m^2, see Table I) is located at the first layer and is equal to 0.78 mJ/m^2 [Fig. 4 (black)]. The second one is due to hybridizations between transition-metal and insulator orbitals (Fe-3d_{z^2} with O-2p_z orbitals) at the interface, mainly in the first layer. This mechanism is active in the case of pure interface and provides the largest total PMA through its contribution from the first Fe layer [Fig. 4 (red)]. Finally, the third one is localized in the second layer from the interface and results from the hybridizations between the Fe-3d orbitals of the first and second layers (first layer 3$d_{xz,yz}$ and 3d_{z^2} with second layer 3d_{xy} and 3$d_{x^2-y^2}$) since the presence of Mg or O vacancies has little effect on this contribution as indicated by the relatively close amplitudes (blue, green, and red bars in Fig. 4). Instead, these vacancies result in decreasing slightly the total interfacial PMA by reducing the contribution from the first layer by about between one-half and one-third compared to the pure case. These second and third mentioned mechanisms lead to the observed enhancement of PMA at the Fe/MgO interface compared to the Fe/vacuum interface. The most dramatic impact on interfacial PMA is in the case of overoxidized interface as seen in Table I. The reason is

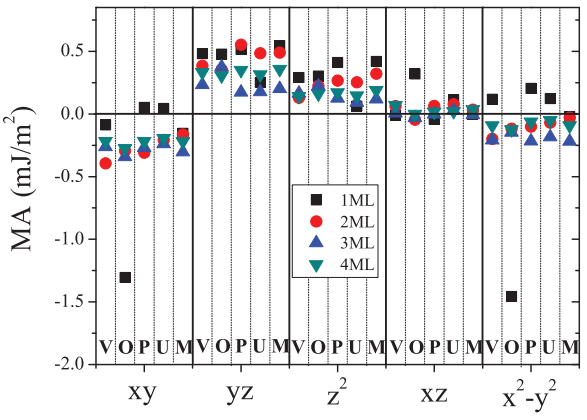

FIG. 5. (Color online) d-orbital resolved contribution to the magnetic anisotropy for different interfacial conditions. V, O, P, U, and M letters correspond to Fe_7/vacuum, overoxidized Fe_7/MgO, pure Fe_7/MgO, underoxidized Fe_7/MgO, and Fe_7/MgO with Mg vacancy case, respectively.

that when oxygen is added to interface 1 in Fe_7/MgO_{11} MTJ [Fig. 1 (O)], a significant abrupt change in PMA occurs where the first-layer contribution becomes negative with a value of -1.7 mJ/m^2 [Fig. 4 (magenta)]. This could be explained by strong in-plane hybridization between Fe-3d and O-2p orbitals (Fe-3d_{xy} and Fe-3$d_{x^2-y^2}$ with O-2$p_{x,y}$) in the FeO layer. Indeed, by looking at the orbital-resolved contribution to the anisotropy shown in Fig. 5, one can see clearly that in the case of overoxidation (O) the contribution of in-plane orbitals (d_{xy} and $d_{x^2-y^2}$) becomes strongly negative in the first layer (black squares) compared to all other cases (V, P, U, M). In fact, analysis of the orbital contribution to the MA shown in Fig. 5 allows to clarify and elucidate even further the microscopic origin of the PMA in Fe/MgO. First, we can see that in general the out-of-plane orbitals (d_{z^2} and $d_{xz,yz}$) always try to align the magnetization out-of-plane while the in-plane orbitals (d_{xy} and $d_{x^2-y^2}$) have a tendency to align the magnetization in plane. Next, the contributions from out-of-plane and in-plane orbitals in the bulk of the layer compensate each other, giving rise to a negligible magnetic anisotropy. However, at the interface, precisely in the first layer, the contribution of the out-of-plane orbitals increases and dominates except for the underoxidized case (U). This concerns especially the contribution from d_{z^2} due to the hybridization with O orbitals in the case of pure (P) and Mg vacancy (M). Interestingly, the in-plane orbitals' contribution (d_{xy} and $d_{x^2-y^2}$) in the first layer in the case of pure and underoxidized interface also tends to align the magnetization in the out-of-plane direction with smaller values compared to d_{z^2} and $d_{xz,yz}$. Finally, the presence of Mg atom at the interface seems to be crucial in changing the in-plane contribution sign from negative to positive. This becomes clear by comparing the pure case with the O and Mg vacancies cases. One can see that while the oxygen vacancies have strong influence on out-of-plane orbital contributions, the Mg vacancies seem to affect only the in-plane ones. This could be related to the fact that the oxygen atom is located on top of the Fe while Mg is located in the hollow site.

In conclusion, using first-principles calculations, we unveiled the microscopic mechanisms of PMA by evaluating the orbital and onsite projected contributions to magnetic anisotropy in Fe/MgO interfaces and MTJs with different interfacial conditions. Our results indicate that the origin of the large PMA observed in MgO-based MTJ is much more complex and richer than described so far by only considering the hybridization between Fe-3d and O-2p orbitals. Furthermore, we demonstrated that the PMA energy is not localized at the interface but also propagates into the bulk of the Fe layers showing a damped oscillatory character as a function of Fe thickness and distance to the interface with a period of 2 ML. This oscillatory character is due to the confinement of minority electrons in $d_{xz,yz}$ orbitals inside the Fe film and between the MgO barrier. It is also found in most situations that states with $d_{yz(xz)}$ and d_{z^2} character tend always to favor PMA, while those with d_{xy} and $d_{x^2-y^2}$ character tend to favor in-plane anisotropy. We expect similar mechanisms may be found in other metal/insulator structures.

We acknowledge D. Apalkov, O. Mryasov, W. H. Butler, P. J. Kelly, and A. Smogunov for fruitful discussions.

*mair.chshiev@cea.fr

[1]K. Mizunuma, S. Ikeda, J. H. Park, H. Yamamoto, H. Gan, K. Miura, H. Hasegawa, J. Hayakawa, F. Matsukura, and H. Ohno, Appl. Phys. Lett. **95**, 232516 (2009).
[2]G. Kim, Y. Sakuraba, M. Oogane, Y. Ando, and T. Miyazaki, Appl. Phys. Lett. **92**, 172502 (2008).
[3]C. Ducruet, B. Carvello, B. Rodmacq, S. Auffret, G. Gaudin, and B. Dieny, J. Appl. Phys. **103**, 07A918 (2008).
[4]J.-H. Park, C. Park, T. Jeong, M. T. Moneck, N. T. Nufer, and J.-G. Zhu, J. Appl. Phys. **103**, 07A917 (2008).
[5]D. Lim, S. Kim, and S. R. Lee, J. Appl. Phys. **97**, 10C902 (2005).
[6]L. E. Nistor, B. Rodmacq, S. Auffret, and B. Dieny, Appl. Phys. Lett. **94**, 012512 (2009).
[7]L. E. Nistor, B. Rodmacq, S. Auffret, A. Schuhl, M. Chshiev, and B. Dieny, Phys. Rev. B **81**, 220407 (2010).
[8]S. Ikeda, K. Miura, H. Yamamoto, K. Mizunuma, H. D. Gan, M. Endo, S. Kanai, J. Hayakawa, F. Matsukura, and H. Ohno, Nat. Mater. **9**, 721 (2010).
[9]M. Endo, S. Kanai, S. Ikeda, F. Matsukura, and H. Ohno, Appl. Phys. Lett. **96**, 212503 (2010).
[10]Yu A. Bychkov and E. I. Rashba, J. Phys. C: Solid State Phys. **17**, 6039 (1984).
[11]I. Zutic, J. Fabian, and S. Das Sarma, Rev. Mod. Phys. **76**, 323 (2004).
[12]P. F. Carcia, A. D. Meinhaldt, and A. Suna, Appl. Phys. Lett. **47**, 178 (1985).
[13]H. J. G. Draaisma, W. J. M. de Jonge, and F. J. A. den Broeder, J. Magn. Magn. Mater. **66**, 351 (1987).
[14]D. Weller, Y. Wu, J. Stöhr, M. G. Samant, B. D. Hermsmeier, and C. Chappert, Phys. Rev. B **49**, 12888 (1994).

[15]S. Monso, B. Rodmacq, S. Auffret, G. Casali, F. Fettar, B. Gilles, B. Dieny, and P. Boyer, Appl. Phys. Lett. **80**, 4157 (2002).
[16]B. Rodmacq, S. Auffret, B. Dieny, S. Monso, and P. Boyer, J. Appl. Phys. **93**, 7513 (2003).
[17]Y. Shita, T. Maruyama, T. Nozaki, T. Shinjo, M. Shiraishi, and Y. Suzuki, Appl. Phys. Express **2**, 063001 (2009).
[18]A. Manchon *et al*., J. Appl. Phys. **104**, 043914 (2008).
[19]G. H. O. Daalderop, P. J. Kelly, and M. F. H. Schuurmans, Phys. Rev. B **41**, 11919 (1990).
[20]K. Nakamura, T. Akiyama, T. Ito, M. Weinert, and A. J. Freeman, Phys. Rev. B **81**, 220409(R) (2010).
[21]M. K. Niranjan, C.-G. Duan, S. S. Jaswal, and E. Y. Tsymbal, Appl. Phys. Lett. **96**, 222504 (2010).
[22]H. X. Yang, M. Chshiev, B. Dieny, J. H. Lee, A. Manchon, and K. H. Shin, Phys. Rev. B **84**, 054401 (2011).
[23]K. H. He, J. S. Chen, and Y. P. Feng, Appl. Phys. Lett. **99**, 072503 (2011).
[24]N. Nakajima, T. Koide, T. Shidara, H. Miyauchi, H. Fukutani, A. Fujimori, K. Iio, T. Katayama, M. Nývlt, and Y. Suzuki, Phys. Rev. Lett. **81**, 5229 (1998).
[25]L. E. Nistor, B. Rodmacq, C. Ducruet, C. Portemont, I. L. Prejbeanu, B. Dieny, IEEE Trans. Magn. **46**, 1412 (2010).
[26]W. C. Tsai, S. C. Liao, H. C. Hou, C. T. Yen, Y. H. Wang, H. M. Tsai, F. H. Chang, H. J. Lin, and Chih-Huang Lai, Appl. Phys. Lett. **100**, 172414 (2012).
[27]A. Manchon, S. Pizzini, J. Vogel, V. Uhlír, L. Lombard, C. Ducruet, S. Auffret, B. Rodmacq, B. Dieny, M. Hochstrasser, and G. Panaccione, J. Magn. Magn. Mater. **320**, 1889 (2008).
[28]G. Kresse and J. Hafner, Phys. Rev. B **47**, 558 (1993); G. Kresse and J. Furthmuller, *ibid*. **54**, 11169 (1996); Comput. Mater. Sci. **6**, 15 (1996).
[29]P. E. Blöchl, Phys. Rev. B **50**, 17953 (1994); G. Kresse and D. Joubert, *ibid*. **59**, 1758 (1999).
[30]Y. Wang and J. P. Perdew, Phys. Rev. B **44**, 13298 (1991).
[31]C.-H. Lambert, A. Rajanikanth, T. Hauet, S. Mangin, E. E. Fullerton, and S. Andrieu, Appl. Phys. Lett. **102**, 122410 (2013).
[32]Similar behavior has been recently reported and attributed to Friedel oscillations by R. Chepulskyy, D. Apalkov *et al*., in the 12th Joint MMM/Intermag Conference, Chicago, 2013 (unpublished) and the International French-US Workshop "Toward low power spintronic devices," La Jolla (2013) (unpublished).
[33]M. D. Stiles, S. V. Halilov, R. A. Hyman, and A. Zangwill, Phys. Rev. B **64**, 104430 (2001).
[34]M. Przybylski, M. Dabrowski, U. Bauer, M. Cinal, and J. Kirschner, J. Appl. Phys. **111**, 07C102 (2012).
[35]U. Bauer, M. Dabrowski, M. Przybylski, and J. Kirschner, Phys. Rev. B **84**, 144433 (2011).
[36]X. J. Wang, H. Zou, and Y. Ji, Phys. Rev. B **81**, 104409 (2010).
[37]The values for $Fe_5[MgO]_3$ can be found in Ref. 22 with $MA_{o,1} + MA_{o,2} = 1.56$, 0.89, and -1.22 mJ/m^2 for P, U, and O cases, respectively.
[38]M. Yamanouchi, R. Koizumi, S. Ikeda, H. Sato, K. Mizunuma, K. Miura, H. D. Gan, F. Matsukura, and H. Ohno, J. Appl. Phys. **109**, 07C712 (2011).
[39]Two of these mechanisms have been also pointed in Ref. 32.